Towards Generalization of Image Anisotropy Analysis

Vassili A.Kovalev
Biomedical Image Analysis Lab, United Institute of Informatics Problems,
Belarus National Academy of Sciences, Surganova St., 6, 220012 Minsk, Belarus
vassili.kovalev@gmail.com

Abstract: *The texture anisotropy is a very important cue for object recognition. Suitable methods and procedures for the analysis of texture anisotropy in 2D images have been developed as early as in mid-eighties of the previous century. These methods were further improved during the early 2000th and successfully adapted for 3D (mostly medical) image analysis. This paper describes work in progress that refers to the third generation of the anisotropy analysis tool. Specifically, it presents a first attempt of generalizing the anisotropy estimation methods based on the very recent ideas of so-called classification gradient and related techniques. These techniques are capitalizing on an extended interpretation of the notion of image gradient treated as any quantitative difference between the two local pixel subsets measured by a suitable method. The approach is illustrated on detecting invisible anisotropy of 3D images of random textures caused by variation of high order statistics.*

***Keywords*:** Anisotropy, 3D image, high-order statistics

1. INTRODUCTION AND LITERATURE SURVEY ON 2D TEXTURE ANISOTROPY

It is commonly accepted in the image processing and pattern recognition community that the texture anisotropy is a very important cue for object recognition. Its importance from the physiological point of view is underlined by the fact that the mammalian vision systems include orientation selective mechanisms in the visual cortex [1,2] and from the psychophysical point of view by the fact that orientation is one of the cues used by humans in the perceptual grouping of patterns [3,4].

The anisotropy estimation methods can be grouped into two categories [5-6]: those that estimate first the local orientation field, perhaps with the help of directional image filtering, and those that operate directly on the image gray values. Most of the methods including the generalized approach introduced in this paper fall under the first category (a number of publications on 2D methods is available but specific references are omitted to keep the size of reference section reasonable).

In order to calculate the local intensity gradient vectors, or to enhance local linear structures and then estimate the anisotropy by considering distribution of local orientations (Fig. 1, central part), various approaches can be explored. For instance, capitalizing on the commonly known Sobel edge detector, A.Y. Sasov (1984, Russia) has provided a very successful implementation of 2D texture anisotropy analysis software. Being integrated with corresponding pieces of imaging hardware and additional software modules, it was commercialized in form of a complete microscopy image analysis tool and sold world-wide under the SasovVISION brand.

During the years 1989-1992, V.A. Kovalev and S.A. Chizhik have been extended this approach to be used for the analysis of anisotropy properties on materials' surface texture on different scale levels (optical, scanning electron, and atomic force microscopy). A special attention in this research was paid to the nanotechnology applications and nano-scale imaging provided by various modes of atomic force/scanning probe microscopes. In particular, the utility of a family of anisotropy histograms computed for different intensity gradient/surface slope levels has been demonstrated (see Fig. 2).

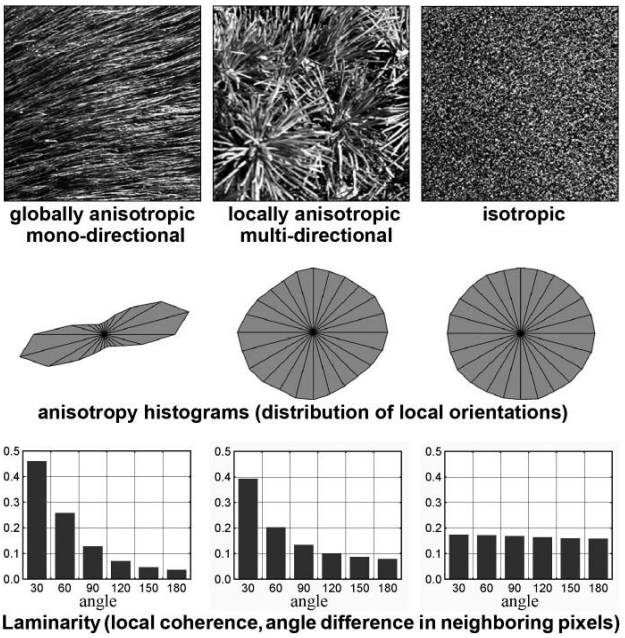

Fig. 1 – Different kinds of 2D texture anisotropy and its measurement using anisotropy histograms and the laminarity (gradient angle co-occurrence) feature.

Later on, similar approaches were further developed by other researchers using steerable filters to estimate local orientation and subsequently they computed a set of typical "orientation maps" (eg., Simoncelli and Farid, 1996). About fifteen years ago (1994), scientists from MIT have suggested to employ steerable pyramids to extract orientation in several scales, for the purpose of performing a quick search in large image databases. They showed that a simple measure, like the "dominant perceived orientation", may suffice for the quick coarse classification of certain kinds of image scenes. For example, it is known that pigeons classify cities and countries in a similar way (Herngstein, 1976). Another example of an efficient use of simple anisotropy feature defined as max-to-min ratio of the anisotropy histogram is detecting tumors in liver ultrasound images (Fig. 3). It is known that ultrasound scanning provides a cheap and convenient way of producing diagnostic images. However, the ultrasound image intensity characteristics are very instable what makes them extremely difficult to analyze using conventional intensity-related texture

analysis approaches. Fig. 3 demonstrates the anisotropy difference for typical regions of normal liver texture and texture with tumor as well as experimental computer-aided diagnosis software developed by the author (1994). As it can be easily seen from the figure, the normal liver texture is better ordered in space and therefore has substantially higher anisotropy value comparing to the regions disturbed by a tumor. Also, the method was further improved by introducing the laminarity (the degree of local gradient vector collinearity) feature defined with the help of 1D angle co-occurrence histogram (see the bottom part of Fig. 1).

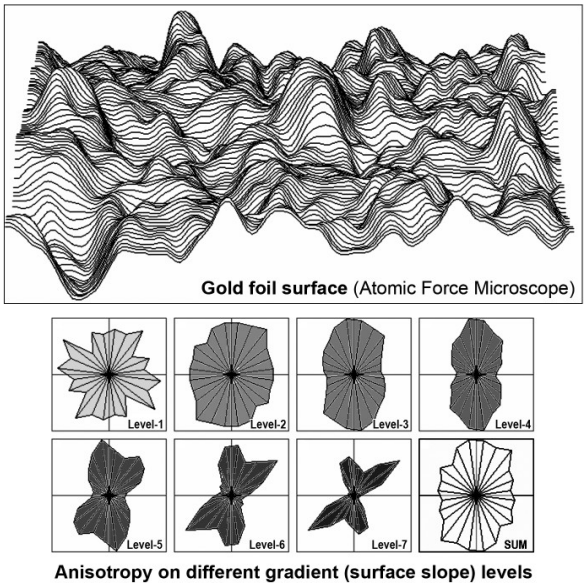

Fig. 2 – Surface nano-scale image and its anisotropy measured on different intensity gradient (surface slope) levels.

The use of multiple scales in orientation estimation may be of crucial importance in scenes where the texture observed is due to the genuine roughness of the surface and the illumination of the scene is variable. Chantler and colleagues have shown in 1994 that the same surface may exhibit different levels of texture and anisotropy when the angle of the incident illumination changes. Ng and Petrou (1992) have used special line enhancement and detection filters to identify the lines and their orientation in finger prints and in seismic sections respectively, before segmenting the images according to the local line orientation. These line filters have been developed under the assumption that isolated lines are to be detected. Thus, when the density of lines is very high, as is the case, for instance, of angiograms and mammograms, the optimal linear filters suffer from interference and fail. Much simpler linear filters have been proved more effective in these cases.

Hasegawa and Toriwaki (1992) assume that the lines have already been extracted and they are dealing with the binary line image in which they characterize local anisotropy by summing the contribution to a certain orientation of all line segments present within a circular neighborhood and weighted inversely proportionally to their distance from the centre. A more sophisticated method of characterizing the local orientation field has been developed in 1993 by Rao for the purpose of fault characterization in semiconductor wafers: The local orientation field is viewed as the phase portrait of a linear map and is classified according to the fixed and singular points of the map matrix. Rao does not assume lines in the image, but simply determines the local orientation field using Gaussian filters.

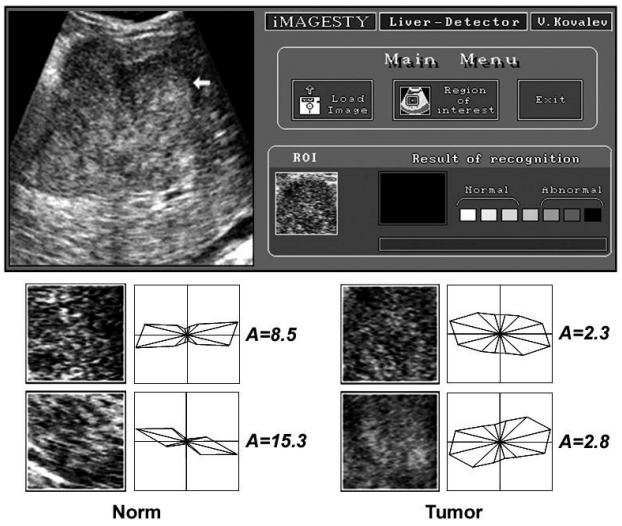

Fig. 3 – Example of the use of 2D anisotropy features for distinguishing tumour area and normal liver texture.

In the second category of methods one should classify all those methods that attempt to estimate local anisotropy directly from the grey image itself. These methods tend to be more robust as they do not rely on the calculation of local derivatives. Several of them have been inspired by the solutions given to the problem of motion estimation. Perhaps the oldest one is the one proposed in 1957 by Longuet-Higgins for the purpose of estimation of spatial roughness distribution on solid surfaces. Heeger's method (1987) formulated as an integral approach, uses spatio-temporal filtering for optic flow estimation and has been used for estimating motion in ultrasound textured images by Cooper and Graham (1996). Sato and Cipolla (1994) used the moments of local texture to perform image registration and estimate surface orientation exploiting the anisotropy induced by projection.

Another important step in further development of 2D texture analysis methods was done in the period of 1981-1995 by Prof. Chetverikov, who has been proposed the use of features extracted from grey level difference histograms (GLDH) for the characterization of anisotropy. For this purpose, GLDH are computed for arbitrary displacements.

2. EXTENDING THE ANISOTROPY ANALYSIS METHODS TO 3D VOLUMETRIC TEXTURES

In the past 10-15 years there was a strong proliferation in sensors that create 3D volumetric images of different modalities, particularly in such specific areas as different kinds of computerized tomography in medicine. There is a need, therefore, to analyze and identify textures in theses images, the same way as it is necessary to deal with textures in 2D images. The analysis of texture anisotropy in medical images is of particular importance for content-based image retrieval (CBIR), classification and pathology diagnosis, while in seismic data, for example, anisotropy analysis may lead to the

identification of seismic horizons which in turn aid the search for oil reserves.

Extension of 2D methods to 3D has largely been confined to the development of 3D edge detectors. Most edge detection methods assume that they are dealing with isolated edges and they cannot cope with the interference caused by the presence of multiple edges. In 1981 Zucker and Hummel have been suggested so-called "optimal" 3×3×3 mask [7]. Since then, several other versions of gradient estimation operators were introduced (eg., Liou and Singh, 1992). However, the simple 3×3×3 operator [7] remains the most frequently used one in practice.

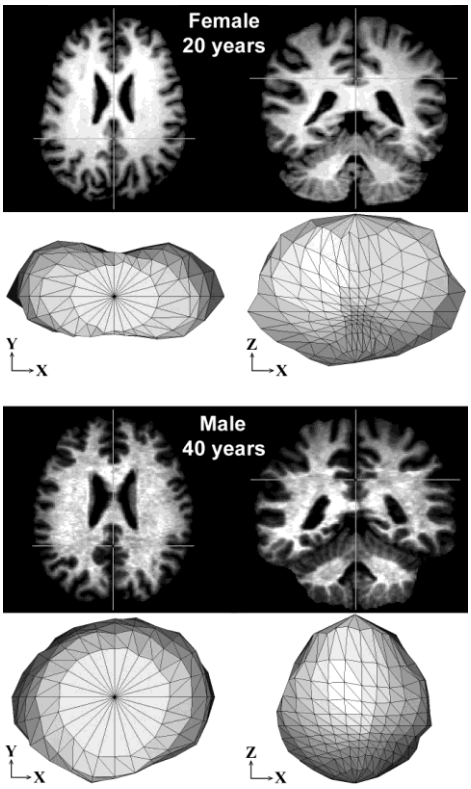

Fig. 4 – Differences of white matter texture anisotropy of the brain associated with age and gender detected using 3D MRI.

Despite the presence of 3D edge detection operators, the pioneering work [8] introducing the anisotropy analysis methods for 3D volumetric images was published only in 1997. After certain improvements and refinements [5, 6] the suggested approach was well accepted by the international image processing community and included in the relatively limited arsenal of 3D texture analysis methods. Two approaches to the characterization of 3D textures were examined in these papers: one is based on gradient vectors and one on extended co-occurrence matrices. They are investigated with the help of simulated data for their behavior in the presence of noise and for various values of the parameters they depend on. They are also applied to several medical volume images characterized by the presence of micro-textures and their potential as diagnostic tools and tools for quantifying and monitoring the progress of various pathologies is discussed. No firm medical conclusions can be drawn as not enough clinical data are available at that time. The gradient-based method appears to be more appropriate for the characterization of micro-textures. It also shows more consistent behavior as a descriptor of pathologies than the extended co-occurrence matrix approach.

Later on, the method has been extensively tested on real problems such as schizophrenia diagnosis based on 3D MRI tomography images [9], quantification of age- and gender-related 3D anisotropy differences of brain's white matter [10] and some other [11, 12]. Fig. 4 provides for examples of 3D anisotropy histograms of brain's white matter computed for two MRI brain images of subjects different in age and gender. It should be stressed that in all the occasions we are dealing with 3D volumetric images whereas Fig. 4 shows only two pairs of orthogonal image slices for clarity. Further details on the white matter anisotropy can be found in [10].

3. GENERALIZED TEXTURE ANISOTROPY ANALYSIS APPROACH: THE BASIC IDEA

The generalized approach for texture anisotropy analysis presented in this paper is referred to the third generation of the anisotropy analysis tool which is currently under development. The approach is substantially based on recent ideas on generalized image gradient and related techniques [13-15]. In its turn, the generalized gradient capitalizes on an extended interpretation of the notion of local image gradient treated as any quantitative difference between the two local pixel subsets (orthogonal window halves) measured by a suitable method. Thus, the major points are:

(a) In order to compute generalized image gradient at each image position, the method makes use the sliding window technique with a spherical (or circular in case of 2D) sliding window of relatively large size consisting of two halves (see the scheme depicted in Fig. 5).

(b) Gradient components *Dx*, *Dy* and *Dz* along the orthogonal image axes X, Y, and Z are calculated as a difference between the subsets of voxels in corresponding window halves.

(c) Depending on the specific image characteristics and the goal of the anisotropy analysis, the quantitative difference between the voxel subsets may be estimated using different methods and computational procedures. In particular, this can be done:

- based on the conventional approach of convoluting voxel values with an enlarged and suitably-weighted 3D or 2D mask,
- using statistical tests (eg., a two-tailed Students's *t*-test) that estimates the statistical difference of voxel subsets and resulted in a well-grounded statistical significance score,
- using suitable voxel classification procedures such as commonly accepted Hierarchical clustering, Support vector machines (SVM) and the Random forests classifiers with subsequent interpretation of the resultant classification accuracy as a measure of difference between voxel subsets (this case we call it the "classification gradient" [14, 15]).

(d) In the majority of cases (except for the conventional convolution approach, which is not of much interest here), the above procedure of calculating quantitative difference between the voxel subsets taken from window halves, may involve statistical bootstrap procedure that rises up the resultant accuracy value for the

price of a very heavy computational load. In order to implement the bootstrap technique, the procedure is modified so that it does not suppose computing voxel difference in one-go on the whole voxel subsets any more. Instead, it includes sub-sampling of a fraction of voxels (say, 50-80%), computing the particular difference, repeating the process for about 100 times and taking the mean difference as an output.

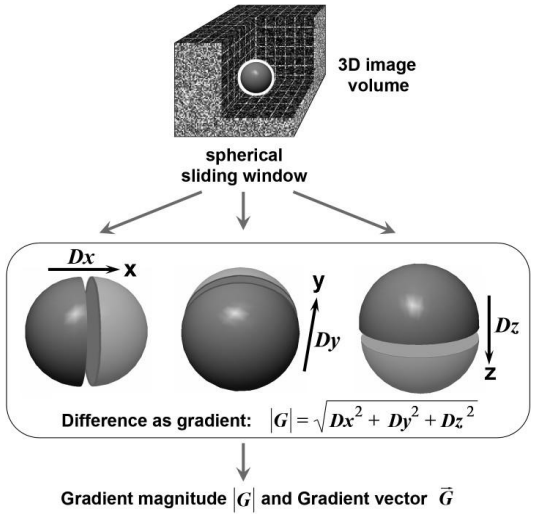

Fig. 5 – Calculating differences between the voxel sets in orthogonal window halves and defining generalized gradient.

Application of the generalized gradient filter to an image produces gradient map with gradient vectors defined for each voxel/pixel position. Once computed, they are used for calculating the anisotropy histogram in a pretty much the same way as it is done in existing 2D and 3D anisotropy analysis methods.

Clearly, introducing the generalized anisotropy analysis, we are primarily aiming to solve the texture analysis problems, which may not be solved by existing methods. Thus, in the sections that follow we present results of experimental evaluation of the method on complicated problems of detecting texture anisotropy that is hardly, if at all, visible for human eye [15, 16].

4. THE TEST IMAGES

A set of synthetic 3D images of random textures was created for testing the method. All test images were of the same size consisting of 256 axial slices with a slice size of 512×512 voxels, 16 bits per voxel. In each image the target texture property (mean, variance and skewness) gradually increased from the upper to the lower slice. Such a design constitute certain texture anisotropy along the vertical image axis *Z* with an inter-slice "gradient" of the examined statistical property directed downwards.

The main test image was presenting random texture with a strong vertical anisotropy which nevertheless remains invisible for human eye. For modeling this property, we capitalized on the fact that two textures *cannot be visually distinguished* in case they have same first and second-order statistics and different in the third-order statistics only [15, 16]. Thus, to create the simulated random textures that differ in their third order moments, we need an asymmetric probability density function that depends on at least two shape parameters.

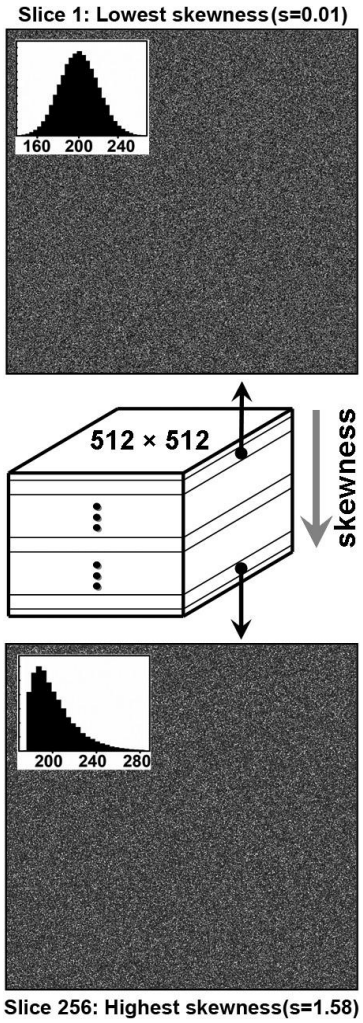

Fig. 6 – 3D test image with invisible anisotropy of random texture directed downwards. The anisotropy is caused by changes of skewness, which gradually increases slice-by-slice.

We have chosen the Gamma distribution which is a two-parameter family of continuous probability distributions. It has a scale parameter Θ and a shape parameter *k* (see Wikipedia). If *k* is an integer then the distribution represents the sum of *k* exponentially distributed random variables, each of which has a mean of Θ. The probability density function of the Gamma distribution can be expressed in terms of the gamma function $\Gamma(k)$ parameterized by the shape parameter *k* and the scale parameter Θ:

$$f(x;k,\Theta) = x^{k-1}\frac{e^{-x/\Theta}}{\Theta^k \Gamma(k)}$$

for $x > 0$ and $k, \Theta > 0$.

In In Gamma distribution the mean *m* (first moment), variance *v* (second moment) and skewness *s* (third moment) are given by the following formulae in terms of the parameters of the distribution:

$$m = k\,\Theta,\ v = k\,\Theta^2,\ s = 2/\sqrt{k}\,.$$

Using the Gamma distribution, the random intensity values of the first test image (see Fig. 6) were generated with the help of R, a language and environment for statistical computing. The skewness parameter started

from the value of s=0.01 for the first slice progressively increasing slice-wise up to the value of s=1.58 for the last axial slice. The mean and the variance of the intensity values remain constant for each slice: m=200, v=400.

Other test images representing 3D random textures with gradually slice-wise increased mean and variance values were created using well known Gaussian distribution which is symmetric that is $s \equiv 0$.

5. DETECTING WEAK INTESITY VARIATION

In order to validate the software implementing suggested method, we start with a simple experiment on evaluating the anisotropy of a test image representing random texture with the intensity gently growing downwards. For this purpose we used Gaussian distribution with the fixed variance and skewness (v=400, s=0 for each of 256 axial slices) and mean values gradually increased form m=200.0 up to m=212.8 with the step as little as Δm=12.8/256=0.05 intensity units per slice.

For this experiment we have chosen to use Student's t-test as the method of calculating differences of voxel subsets taken from sliding window halves. It should be stressed that since the degree of freedom for t-test (number of voxels in window halves) remains constant for all the comparisons, there was no need for normalization of resultant statistical scores. Thus, in each window position the "gradient" of t-value was calculated in a straightforward way based on the three particular values t_X, t_Y, and t_Z obtained for orthogonal image axes.

The anisotropy evaluation procedure was repeated 4 times with the radius of spherical sliding window R = 5, 10, 15 and 20 voxels. In addition, the existing ("conventional" for short) method of 3D texture anisotropy analysis was also applied for comparative purposes. In all the occasions anisotropy histograms were visualized and the anisotropy features *F1* (max-to-min histogram ration), *F2* (deviation of the histogram from sphere, or *integral anisotropy*) and *F3* (local histogram roughness) calculated as described in [5, 6] to enable quantitative comparisons. Results of all five experiments are summarized in Table 1. Example of anisotropy histograms is provided in Fig. 7 (R = 15).

Table 1. Anisotropy of texture with increasing intensity

Method, Window radius	*F1*	*F2*	*F3*
Conventional	1.0	*0.1*	0.2
Generalized, R=5	1.6	*0.4*	0.3
Generalized, R=10	10.2	*6.7*	1.6
Generalized, R=15	482.8	*17.2*	17.2
Generalized, R=20	2821.0	*30.9*	64.7

As it can be seen from Table 1 and Fig. 7, being applied to the first test image with very weak vertical intensity anisotropy, the conventional method fails to detect any directional structure in given random texture image (*F1*=1.0, anisotropy histogram is pretty similar to sphere).

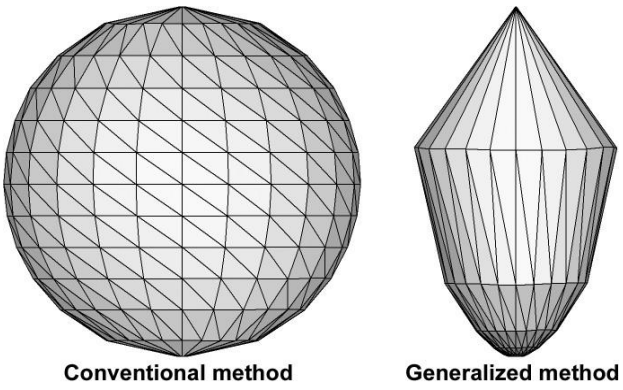

Fig. 7 – Anisotropy histograms of 3D random texture image with a weak vertical anisotropy.

In the same time, the generalized approach captures these subtle statistical intensity changes in vertical direction relatively easy.

6. DETECTING INVISIBLE ANISOTROPY

Experiments on detecting invisible anisotropy were performed using 3D test image illustrated in Fig. 6. According to the theory, since the inter-slice differences are only concerned with the third-order statistics, they should not be visible at all, even when comparing the most distinct bordering slices depicted in Fig. 6 (some subtle differences may be noted due to the technical picture printing imperfections). In addition, one should also remember about the extremely weak inter-slice changes of the intensity skewness parameter, which is as weak as Δs=(1.58-0.01)/256=0.006.

For calculating dissimilarity of the voxel subsets in halves of sliding window, we have employed the optimal for this case technique consisting of calculating the skewness of two distributions and taking their difference. Similar to the previous experiment, five runs were performed, one based on the conventional method and the rest four using generalized anisotropy analysis with the varying sliding window radius. Experimental results on the anisotropy quantification are summarized in Table 2. Fig. 8 shows resultant anisotropy histograms viewed from a fixed point located at (30, -30) degrees of rotation along the longitude and latitude respectively (the anisotropy histogram produced by conventional approach is omitted because it is simply spherical).

Table 2. Anisotropy of texture with increasing skewness

Method, Window radius	*F1*	*F2*	*F3*
Conventional	1.0	*0.0*	0.2
Generalized, R=5	2.0	*1.4*	3.6
Generalized, R=10	4.7	*4.4*	1.3
Generalized, R=15	47.3	*11.1*	6.1
Generalized, R=20	1292.0	*21.4*	32.2

From the data given in Table 2 and illustrated in Fig. 8, it can be concluded that the method is capable of detecting invisible anisotropy in 3D random texture images.

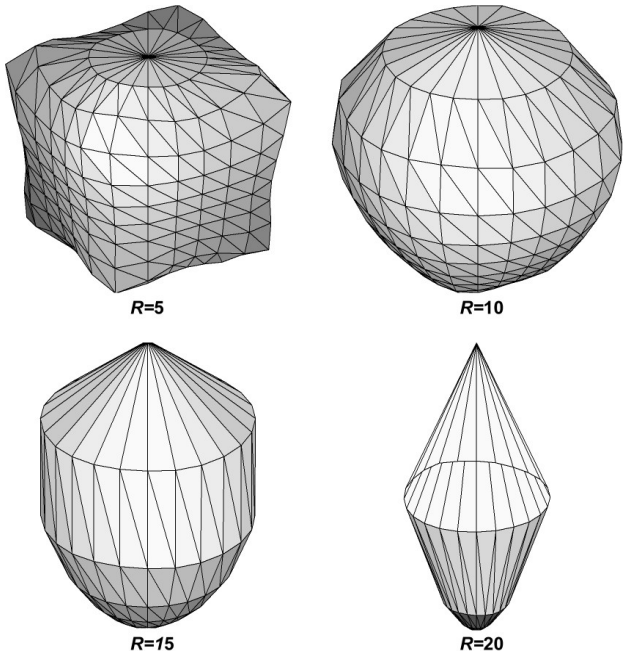

Fig. 8 – Anisotropy histograms of 3D random texture image with invisible anisotropy computed with different radiuses *R*.

7. CONCLUSIONS

This paper has presented the first attempt on the development of third generation of the image anisotropy analysis tool. The approach suggested in the paper was based on very recent ideas of so-called generalized gradient and related techniques introduced by author a bit earlier. These techniques are capitalized on an extended interpretation of the notion of image gradient treated here as any quantitative difference between the two pixel subsets involved into calculation of local gradient with the help of suitably-sized sliding window. Introducing the generalized anisotropy analysis, we were primarily aiming to solving the texture analysis problems, which may not be solved by existing methods. In order to achieve this, we have performed experimental evaluation of the method on complicated problems of detecting 3D texture anisotropy that is hardly, if at all, visible for human eye. From the results reported with this pilot study, it can be concluded that the method is capable of such problems and therefore the mission of this very first study is accomplished.

The suggested approach has several advantages over the existing methods of 2D and 3D anisotropy analysis. In particular, when computing generalized gradient, any window size can be specified according to the specific anisotropy analysis task without any changes of the method and its software implementation. Another strong point is that a possibility of using statistical bootstrap technique is arising with all the accuracy benefits this statistical procedure provides. Among disadvantages of the method is only the high computational cost.

Acknowledgements **–** This work was funded by the ISTC grant B-1489 and partly by the grant IJP 2006/R1 of the British Royal Society.

REFERENCES

[1] D.H. Hubel, T.N. Wiesel. Receptive fields, binocular interaction and functional architecture in the cat's visual cortex, *Journal of Physiology*, 166 (1962), pp. 106-154.

[2] D.H. Hubel, T.N. Wiesel. Receptive fields and functional architecture of monkey striate cortex, *Journal of Physiology*, 195 (1968), pp. 215-243.

[3] B. Julesz. Experiments in visual perception of texture, *Scientific American*, 232 (1975), pp 34-43.

[4] A.R. Rao, G.L. Lohse. Identifying high level features of texture perception, *CVGIP: Graphical Models and Image Processing*, 55 (1993), pp. 218-233.

[5] V.A. Kovalev, M. Petrou, Y.S. Bondar. Texture anisotropy in 3D images, *IEEE Transactions on Image Processing*, 8 (3) (1999), pp. 346-360.

[6] Kovalev V.A. and Petrou M. Texture analysis in three dimensions as a cue to medical diagnosis, book chapter in *Handbook of Medical Imaging: Processing and Analysis*, I.Bankman (Ed.), Academic Press, San Diego, CA, USA (2000), pp. 231-247.

[7] S.W. Zucker, R.A Hummel. A 3D edge operator, IEEE Transactions on *Pattern Analysis and Machine Intelligence*, 3 (1981) 324-331.

[8] Kovalev V.A., Bondar Y.S. A method for anisotropy analysis of 3D images, *Proceedings of the 7th International Conference On Computer Analysis of Images and Patterns (CAIP'97)*, Kiel, Germany, 10-12 September 1997, LNCS, vol. 1296, Springer Verlag, pp. 495-502.

[9] V.A. Kovalev, M. Petrou, J. Suckling. Detection of structural differences between the brains of schizophrenic patients and controls, *Psychiatry Research: Neuroimaging*, 124 (2003), pp. 177-189.

[10] V. Kovalev, F. Kruggel. Texture anisotropy of the brain's white matter as revealed by anatomical MRI. *IEEE Transactions Medical Imaging*, 26(5) (2007), pp. 678-685.

[11] V.A. Kovalev, F. Kruggel, H.-J. Gertz, D.Y. von Cramon. Three-dimensional texture analysis of MRI brain datasets, *IEEE Transactions on Medical Imaging*, 5 (20) (2001). pp. 424-433.

[12] V.A. Kovalev, F. Kruggel, D.Y. von Cramon. Gender and age effects in structural brain asymmetry as measured by MRI texture analysis, *NeuroImage*, 19, (2003), pp. 896-905.

[13] V.A. Kovalev, M. Petrou. Invisible differences in brain images of schizophrenics and controls. *Proceedings of Medical Image Understanding and Analysis Conference (MIUA-2004)*, Imperial College, London, 23-24 September 2004, D. Rueckert, J. Hajnal and G.-Z. Yang (Eds.), pp. 109-112.

[14] V.A. Kovalev, M. Petrou. The classification gradient. *International Conference on Pattern Recognition (ICPR-2006)*, Hong Kong, 20-24 August 2006, vol. 3, IEEE Computer Society, ISSN 1051-4651, pp. 830-833.

[15] В.А. Ковалев. Метод вычисления обобщенного градиента для текстурных изображений, Информатика, 3 (2008), с. 56-69.

[16] M. Petrou, V. Kovalev, J. Reichenbach. Three-dimensional nonlinear invisible boundary detection. *IEEE Transactions on Image Processing*, 15(10) (2006), pp. 3020-3032.